Energetic connectivity creates heterogeneity of PS II centres in plants probed by the fluorescence rise O-J-I-P : fitting of experimental data to three different PS II models

Strasser, Reto; Stirbet, A.D.

Integrated Plant Systems
H. Greppin *et al.*, eds.
University of Geneva, pp. 81-93

Energetic connectivity creates heterogeneity of PS II centres in plants probed by the fluorescence rise O-J-I-P. Fitting of experimental data to three different PS II models

R.J. STRASSER[1] & A.D. STIRBET[1,2]

[1]*Bioenergetics Laboratory, University of Geneva, CH-1254 Jussy-Geneva, Switzerland*
Tel: +41 22 759 19 44; Fax: +41 22 759 19 45; E-mail: strasser@uni2a.unige.ch,
http://www.come.to/bionrj
[2]*Biophysics Department, University of Bucharest, R-76900 Bucharest, Romania*

Abstract

In presence of DCMU, the sigmoidicity of Chl *a* fluorescence induction curve is correlated to the energetic connectivity (grouping) between photosynthetic units PS II. We are using the experimental data of the fluorescence transients without DCMU (i.e., the O-J-I-P fast fluorescence induction curves) to calculate the overall probability '*p*' of PS II connectivity of the samples (e.g., leaves or chloroplasts). The values obtained using the same method on DCMU treated samples give very close results. Beside the practical advantage of the quantitative determination of the grouping probability on plants from O-J-I-P fluorescence transients, we also present a possible role of the regulation of the connectivity process in photosynthesis as a response to external perturbations. A theoretical discussion based on numerical simulation and fitting of the experimental data, shows three different possible approaches of the fluorescence signal. All are deduced from the same reaction scheme of the acceptor part of PS II centre, involving the primary acceptor pheophytine (Ph), the two bound quinones (Q_A and Q_B), and the plastoquinone pool. The fraction of closed reaction centres *B(t)*, responsible for the fluorescence transient, is calculated using different definitions as distinct combinations of the redox components for every case. The fluorescence rise of two models is based on the conventional assumption, that the presence of Q_A^- determines the high fluorescence state, and one model is based solely on the photochemical charge separation in the reaction centre complex. The transformation of a fluorescence induction curve into a kinetic of the fraction of closed reaction centres is a precondition for the simulation and fitting of biochemical models with experimental data.

1. Introduction

The fluorescence intensity of chlorophyll (Chl) in plants, algae and cyanobacteria depends on the state of the PS II reaction centres [4]. In terms of the quencher theory

of Duysens & Sweers [3], the fast polyphasic fluorescence rise from a minimum F_0 to a maximum value F_P (= F_M in saturating light) is mainly due to the photoreduction of the fluorescence quencher, the primary acceptor Q_A to its nonquenching form, Q_A^-.

The excitation energy transfer among PS II units, commonly denoted as PS II connectivity [7], or grouping [16], also influences the shape of the induction curve. The quantitative relation between the relative variable fluorescence, $V(t) = [F(t)-F_0]/(F_M - F_0)$, and the fraction of PS II with reduced Q_A (closed centres), $B(t)$, has a hyperbolic form, and is described by the well-known equation for the fluorescence behaviour of PS II units as derived by Strasser in 1978 and later [16,17]:

$$V(t) = \frac{B(t)}{1 + C[1 - B(t)]} \tag{1}$$

with:

$$C = p\frac{F_M - F_0}{F_0} \tag{2}$$

where C is the parameter for the curvature of the hyperbola, and p is the overall probability of connectivity between the PS II units. Lavergne & Trissl [9] have also derived in 1995 identical equations, based on the radical pair model. The formulae have been established for single turn over situations (e.g., in presence of DCMU), when Q_A is reduced only once, and the fluorescence transient has an O-J shape, with $F_J \equiv F_M$, but it is considered valable also for the multiple turn over situations.

According to Eq. (1), for unconnected photosystems (e.g. with $C = p = 0$) the relative variable fluorescence is identical to the fraction of closed reaction centres. Therefore, considering a homogeneous PS II population, the kinetics of a fluorescence transient in presence of DCMU becomes exponential:

$$V_E(t) = B_E(t) = 1 - e^{-k(t-t_0)} \tag{3}$$

where k is the rate constant of Q_A reduction and the rate constant of fluorescence rise in the same time. Unfortunately, for the normal transients (e.g. without DCMU) we cannot determine the curvature constant C using Eq. (1), as $B(t)$ is unknown. Here, we will present an original semiempirical method to evaluate C (and then p) using the starting part of curve $V(t)$. This method was used to calculate C and p for both, normal and DCMU treated pea leaf. The results have been discussed and compared with those obtained from numerical simulation of O-J-I-P transients [13].

2. Material and Methods

Experiments were done *in vivo*, with mature intact pea (*Pisum sativum*) leaves. In DCMU treatment, a droplet of 500 µl of DCMU solution (170 µM in distilled water) was added on the axial side of the leaf and kept in the dark for 24 hours. Fluorescence induction transients were measured at room temperature, with a shutter-less fluorimeter (Plant Efficiency Analyser, built by Hansatech Ltd.).

The dark-adapted samples were illuminated for one second with continuous light (600 Wm^{-2}, emission peak at 650 nm) provided by an array of six light-emitting diodes, focussed on a circle of 4 mm diameter of the sample surface. The fluorescence

signals were detected using a PIN-photodiode after passing through a long-pass filter (50% transmission at 720 nm). The first reliable point of the transient is measured at t_0 = 0.05 ms after the onset of illumination, and was taken as F_0.

3. Result and Discussion

Under high light, typically over 500 Wm^{-2}, two intermediate steps designated as F_J (the "J" level; at 2 ms) and F_I (the "I" level; at 30 ms) normally appear in the transient [18] (see *curve 1* in Figure 1). After DCMU treatment the fluorescence rises quickly to its maximum value, F_M, at a time close to that of F_J in the normal curve (see *curve 2* in Figure 1). Numerical simulations of fast fluorescence induction curves [12,14] have shown that the O-J part of the O-J-I-P transient is mainly due to first reduction of Q_A. Therefore, O-J rise is very similar to the transient measured on DCMU treated leaves, in which the Q_B site is occupied by a DCMU molecule, and the transfer of electron from Q_A to Q_B is interrupted. Moreover, it has been shown [15] that the shape of the O-J part of a normal transient (t < 2 ms) measured *in vivo* is quite proportional to the O-J rise in the presence of DCMU.

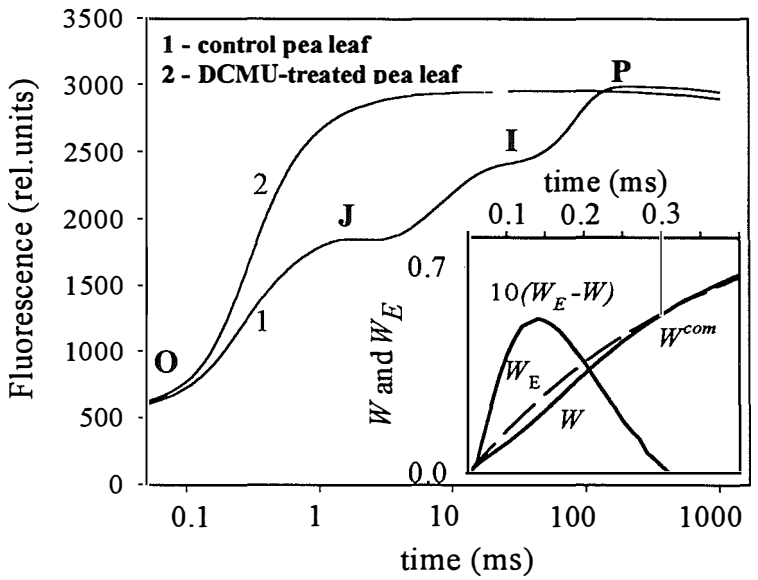

Figure 1. Fast fluorescence induction kinetics of a normal pea leaf (*curve 1*), and of a DCMU-treated pea leaf (*curve 2*), measured in high light (see Material and methods for the experimental conditions)

Insert: *Curve W*: normalised O-J part of *curve 1* presented until 0.4 ms, on a linear time scale; *Curve* W_E: theoretical *exponential curve* corresponding to the unconnected system (see the text); W^{com}: the intersection point of the curves W and W_E (common point); *Curve* $10(W_E-W)$: the difference (W_E-W) multiplied 10 times.

So, we normalise the O-J part of $V(t)$ at V_J as asymptote:

$$W(t) = \frac{V(t)}{V_J} = \frac{F(t) - F_0}{F_J - F_0} \tag{4}$$

The resulting curve (see curve W in the Insert of Figure 1) will be considered as a sigmoidal DCMU transient. $W(t)$ can also be calculated by an equation similar to (1):

$$W(t) = \frac{B^W(t)}{1 + C^W[1 - B^W(t)]} \tag{5}$$

where C^W is the curvature constant of the hyperbola $W(t)$, and $B^W(t)$ is the fraction of closed PS II centres relative to the fraction of PS II centres closed at V_J (due to the normalisation of the curve $F(t)$ at F_J). The curvature constant C^W is correlated with the curvature constant C of the original transient $V(t)$, and the overall probability of connectivity between PS II units in the original system p, by the relationship:

$$C^W = CV_J = p\frac{F_M - F_0}{F_0}V_J \tag{6}$$

also considering the double normalisation of the original fluorescence transient, and the Eq. (2).

Now, we will consider an hypothetically unconnected system similar to those related to $W(t)$, which can be described by an exponential curve (see Eq.(3)):

$$W_E(t) = B_E^W(t) = 1 - e^{-k(t-t_0)} \tag{7}$$

where $B^W{}_E(t)$ is the fraction of closed PS II units corresponding to this hypothetical unconnected system.

We have shown theoretically [12] that DCMU transients for different values of C intersect the hypothetical exponential transient corresponding to the unconnected system in a quite narrow region, which can be approximated with a point. We have applied this observation in our case, constructing graphically the exponential curve $W_E(t)$ (see the dashed curve W_E in the Insert of Figure 1). Both curves, $W(t)$ and $W_E(t)$, have one common point $W^{com} = W_E{}^{com}$ beside the origin, and the same asymptote V_J. The value of the rate constant of the exponential fluorescence rise k can be calculated using the relations (7) and (4), as:

$$k = -\frac{1}{t_{com} - t_0}\ln(1 - W^{com}) = \frac{1}{t_{com} - t_0}\ln\frac{F_J - F_0}{F_J - F_{com}} \tag{8}$$

The fluorescence rise of the unconnected PS II system can be calculated then as:

$$W_E(t) = 1 - e^{-k(t-t_0)} = 1 - \left(1 - W^{com}\right)^{\frac{t-t_0}{t_{com}-t_0}} = 1 - \left(\frac{F_J - F_{com}}{F_J - F_0}\right)^{\frac{t-t_0}{t_{com}-t_0}} = B_E^W(t) \tag{9}$$

We have studied the k value as a function of the position of the common point W^{com}, for both normal and DCMU transients (see Figure 2, solid and dashed curves). Note that we have used the same asymptote (V_J at 2 ms) also for the case in presence of DCMU. It appears that k is quite constant in an interval starting from 0.3 ms to 0.9 ms.

We choose 0.3 ms to calculate k by the common point (t^{com},W^{com}).

Knowing k, one can calculate the hypothetical exponential curve $W_E(t)$ at any time according to the Eq.(7). The difference between the two curves, W_E - W = ΔW (see the Insert of Figure 1) shows the effect of energetic connectivity (grouping) between photosynthetic units on the fluorescence transient. At the time corresponding to the maximal value of ΔW we consider to have the best experimental resolution to calculate the hyperbola parameter C^W of Eq. (5).

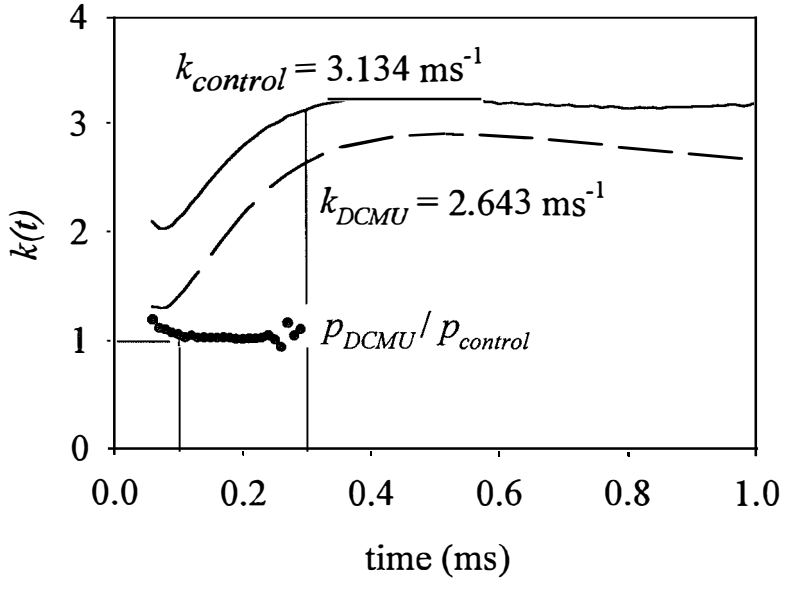

Figure 2. The exponential constant k for normal control (solid curve) and DCMU-treated leaves (dashed curve) as a function of the common point (W^{com}) position considered in the calculus (see Eq. (8)); The ratio of the overall probabilities of connectivity between PS II units, calculated for DCMU treated and normal control leaves, $p_{DCMU}/p_{control}$, is represented by points (see the text for details).

The relative variable fluorescence $W(t)$ and $W_E(t)$ are expressed as functions of the fraction of closed reaction centres $B^W(t)$ and $B^W{}_E(t)$ (see (5) and (7). For the small starting time interval of the transient, until 0.3 ms, we will approximate:

$$B^W(t) = B^W{}_E(t) = W_E(t) \tag{10}$$

Therefore, the curvature constant C^W of the hyperbola $W(t)$ can be calculated considering successively the Eqs. (5) and (10), as:

$$C^W = \frac{B^W - W}{W(1-B^W)} = \frac{W_E - W}{W(1-W_E)} \tag{11}$$

We have calculated W_E in Eq. (11) according to Eq. (9), by setting the time at a position of high sensitivity, $t = 0.1$ ms.

Finally, the overall probability of connectivity between PS II units, p, is calculated using Eq. (6) as:

$$p = C\frac{F_0}{F_M - F_0} \tag{12}$$

The users of this equation have to keep in mind that the fluorescence intensities F_0 and F_M have to originate from PS II antenna only. If this is not the case for a given sample, a deconvolution of experimental F_0 = F_0 (PS II) + F_0 (non-PS II) becomes necessary.

In Table 1 the estimations of the curvature constant C, and the probability of energy transfer among PS II units p, for both normal (control) and DCMU-treated pea leaves, have been presented. We have considered W^{com} at 0.3 ms for k, and W and W_E at 0.1 ms for C in the calculations. The obtained values for both cases are very close: $C_{control}$ = C_{DCMU} = 0.98, $p_{control}$ = 0.25 and p_{DCMU} = 0.26. Moreover, the ratio of $p_{DCMU}/p_{control}$ as a function of the time used in the evaluation of C is close to 1 (the curve represented by points in Figure 2), which can be considered as a confirmation of the method presented here.

Table 1. The values of experimental and theoretical parameters used in the calculations, as well as the resulted values of the curvature constant C, and the overall probability for energy transfer among PS II units p, obtained from the fast fluorescence induction data measured on normal (control) and DCMU-treated pea leaves.

	F_0	F	F^{com}	F_J	F_M	V_J	W	W^{com}	W_E	k	C^W	C	p
ms	*0.05*	*0.1*	*0.3*	*2*	*max*	*2*	*0.1*	*0.3*	*0.1*	*0.3*			
control	604	730	1283	1854	2992	0.523	0.101	0.543	0.145	3.13	0.51	0.98	0.25
DCMU	626	777	1696	2839	2963	0.947	0.068	0.483	0.124	2.64	0.93	0.98	0.26

Another confirmation of the present method to calculate the curvature and connectivity parameters, C and p, has been obtained in the numerical simulation study of the fluorescence induction transient O-J-I-P [13]. In this work we obtained the values of C and p by fitting the experimental fluorescence induction data measured on a normal pea leaf with the mathematical model of the fast fluorescence induction process presented in [12]. Even if the two methods have very different theoretical approaches, the fitted values of these two parameters have been close to those presented here (i.e. $C_{control}$ = 0.8 and $p_{control}$ = 0.2).

However, we must note that the method to estimate *in vivo* the probability of energy transfer between photosynthetic units can be viewed in several ways, depending on the initial hypothesis. We have considered previously the quencher theory of Duysens & Sweers [3], published as early as 1963, in which the fluorescence rise is attributed to the photoreduction of the fluorescence quencher, the quinone acceptor Q_A, to its nonquenching form, Q_A^-. This theory is considered generally as a dogma by the majority of the researchers working in the fluorescence induction field. However,

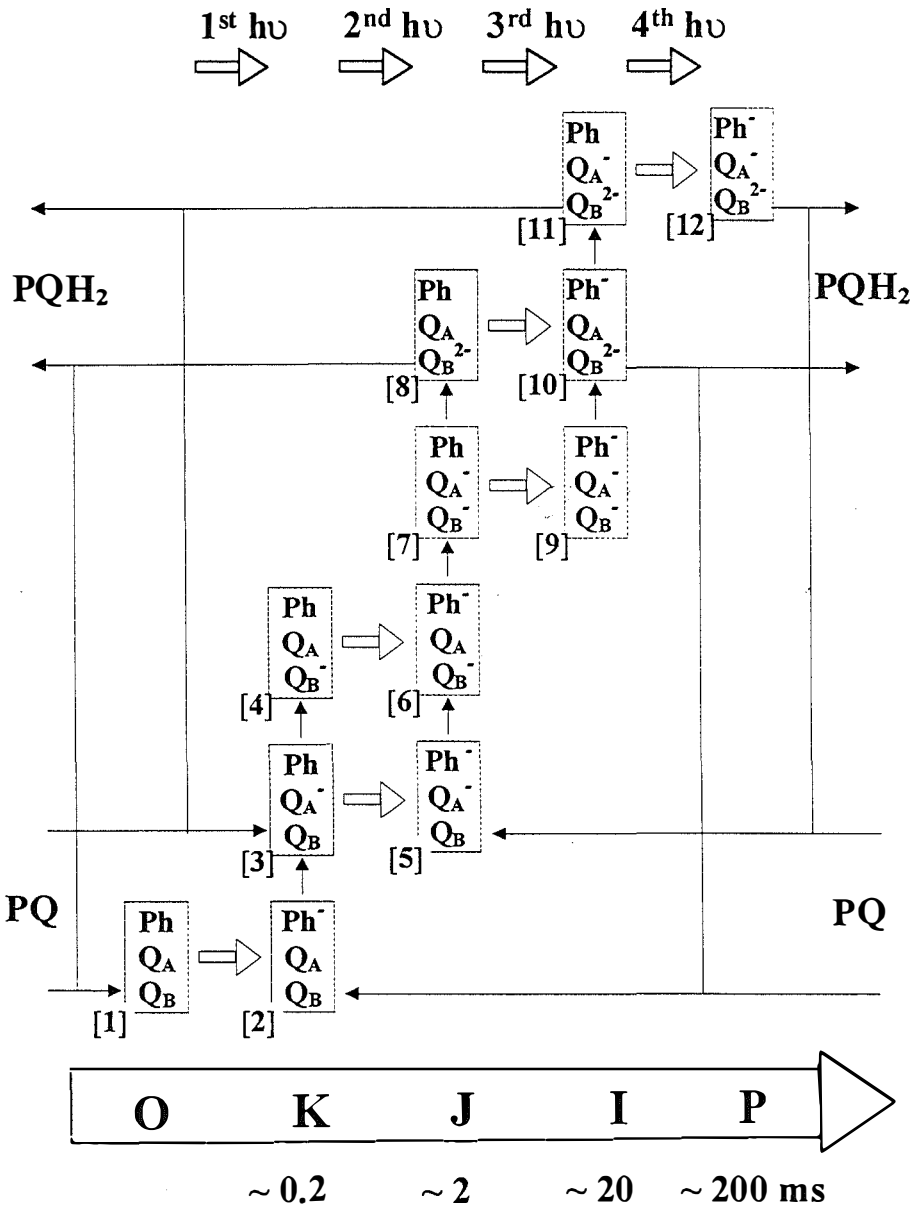

Figure 3. The reaction scheme of the electron transfer reactions at the acceptor side of PS II reaction centre. Four light quanta are necessary for the complete reduction of the electron carriers (PhQ_AQ_B). The K-J-I-P phases of the fluorescence transient are correlated with the accumulation of electrons in PS II unit, but not in a very strict sense, depending on the definite case (see Figure 4 a, b and c).

during the last forty years, our knowledge regarding the composition and the structure of PS II has been completed with a lot of information [2]. For example, the redox state of Pheophytine (Ph), identified much later as the first acceptor of PS II [1], can also be considered in the model (see the reaction scheme in Figure 3). There are several ways to do that, and we will briefly present them here.

(a) Considering Ph^- states in the 'classical' model, in which Q_A^- acts as quencher (hypothesis of Duysens & Sweers [3]). The fraction of PS II closed centres, B, will be calculated as:

$$B = PhQ_A^-Q_B + Ph^-Q_A^-Q_B + PhQ_A^-Q_B^- + Ph^-Q_A^-Q_B^- + PhQ_A^-Q_B^{2-} + Ph^-Q_A^-Q_B^{2-} \quad (13)$$

(b) Considering Ph^- responsible for the fluorescence rise (i.e. due only to the photochemical closing of the centres), instead to a hypothetical quenching action of Q_A^- (hypothesis of Strasser & Stirbet). The fraction of PS II closed centres, B, will only be dependent on the presence of Ph^-, and it will be calculated as:

$$B = Ph^-Q_AQ_B + Ph^-Q_A^-Q_B + Ph^-Q_AQ_B^- + Ph^-Q_A^-Q_B^- + Ph^-Q_AQ_B^{2-} + Ph^-Q_A^-Q_B^{2-} \quad (14)$$

(c) Considering Ph^- states in the 'classical' model, but supposing a double contribution to the fluorescence rise of the centres with both, first and second electron acceptors (i.e. Ph and Q_A) reduced (hypothesis by W.I. Vredenberg, [19]). The fraction of PS II closed centres, B, will be calculated as:

$$B = (1/2)(PhQ_A^-Q_B + PhQ_A^-Q_B^- + PhQ_A^-Q_B^{2-}) + Ph^-Q_A^-Q_B + Ph^-Q_A^-Q_B^- + Ph^-Q_A^-Q_B^{2-} \quad (15)$$

These different models have been tested by numerical simulation and fitting, with experimental data measured on camellia leaf, by using the software Gepasi [10]. The fitting procedure for parameter optimisation was a direct search method [6]. The curvature constant of the fluorescence transient measured on camellia leaf was estimated with the method presented in this paper: $C = 0.6828$ (corresponding to an overall probability of the connectivity between PS II units of $p = 0.17$). We have used this value for theoretical calculation of the relative variable fluorescence, $V(t)$, conforming to Eq. (1). The fraction of closed centres, $B(t)$, has been calculated for every model differently, using the relationships (13), (14) and (15).

The experimental fluorescence induction data are quite well fitted by all of these three models, as it can be seen in Figures 4 a, b, and c respectively. However, the models differ essentially in the relative contribution of different redox forms of the reaction centres (labelled from 1 to 12 in the reaction scheme presented in Figure 3) to the variable fluorescence.

In the first model (the case 'a'), based on the concept that Q_A^- is responsible for the high fluorescence yield, all the six redox forms which contribute to $B(t)$ (i.e. 3, 5, 7, 9, 11, and 12 – see relation (13) and Figure 3) are present in a non-negligible concentration, and have their own kinetics during the O-J-I-P fluorescence rise (see Figure 4 a).

For the second model (the case 'b'), which is based on a very different concept than the first one, we have assumed that the redox state of Q_A alone is not influencing the fluorescence yield. The change in fluorescence yield is proposed to depend only on the

photochemical quenching in a classical way, due to the primary photochemical activity. Therefore, the six components due to the reduced state of Ph (i.e. 2, 5, 6, 9, 10, and 12 – see relation (14) and Figure 3) can contribute to the variable fluorescence.

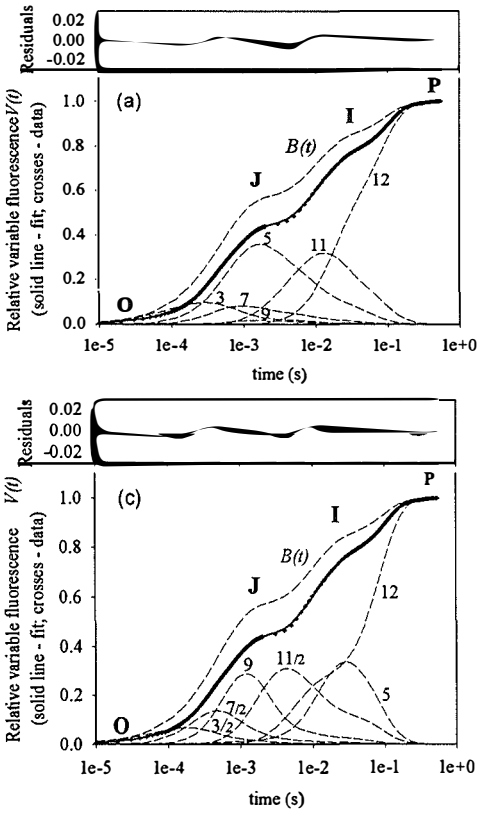

Figure 4. The results of the fit of Chl a fast fluorescence induction curve measured *in vivo* on Camelia leaves (see Material and Methods) with the model presented in Figure 3. With the three different cases a, b, and c for the computation of the fraction of PS II closed units *B(t)* (see the text, relationships (13)-(15)) we have obtained three distinctive constellations of redox components, respectively.

It is highly interesting to see that after the fitting procedure only two forms dominate the induction kinetics nearly entirely: $Ph^{-}Q_A^{-}Q_B$ and $Ph^{-}Q_A^{-}Q_B^{2-}$ (see Figure 4 b).

The third model (the case 'c') is a pondered mixed case between the first two models 'a' and 'b'. As in the first model, Q_A^{-} is responsible for the increase of the fluorescence yield, but the redox forms in which also Ph is in the reduced state have a higher one (W.I. Vredenberg assumed that the fluorescence yield is double, [19]). As for the first model, all six components (i.e. 3, 5, 7, 9, 11, and 12 – see relation (15) and Figure 3) appear clearly in the fit of the experimental curves, but with different kinetics (see Figure 4 c).

Table 2. Values of the optimised kinetic constants of the light reactions $k_L(i)$ (with '*i* ' denoting the number of electrons transferred on the reaction centre PS II) comparatively for the three models (a, b, and c). The electron transfer reactions presented in the table are (see Figure 3): ***R1***: [1]→[2]; ***R4***: [3]→[5]; ***R6***: [4]→[6]; ***R9***: [7]→[9]; ***R11***: [8]→[10]; and ***R13***: [11]→[12].

Model	$k_L(1)$ s^{-1}	$k_L(2)$ s^{-1}	$k_L(3)$ s^{-1}	$k_L(4)$ s^{-1}
a	*R1*:1.11e+03	*R4*: 5.43e+03 *R6*: 3.34e+04	*R9*: 7.17e+02 *R11*: 7.85e+01	*R13*: 1.02e+02
b	*R1*: 2.30e+04	*R4*: 1.45e+03 *R6*: 2.02e+08	*R9*: 3.05e+05 *R11*: 1.09e+01	*R13*: 1.76e+02
c	*R1*: 2.32e+03	*R4*: 1.45e+02 *R6*: 9.32e+04	*R9*: 2.29e+03 *R11*: 7.36e+01	*R13*: 8.67e+01

Table 3. Values of the optimised kinetic constants of electron transfer reactions between Ph, Q_A, Q_B, and PQ pool (see the reaction scheme in Figure 3) comparatively for the three models (a, b, and c) and the references from the literature. In the last colon is presented the standard deviation of the fitting. The electron transfer reactions presented in the table are (see Figure 3): ***R2***: [2]→[3]; ***R3***: [3]→[4]; ***R5***: [5]→[6]; ***R7***: [6]→[7]; ***R8***: [7]→[8]; ***R10***: [9]→[10]; ***R12***: [10]→[11]; ***R14***: [8]→[1]; ***R15***: [10]→[2]; ***R16***: [11]→[3]; and ***R17***: [12]→[5].

Model	k_{Ph} s^{-1}	k^1_{AB} s^{-1}	k^2_{AB} s^{-1}	k_E $s^{-1}M^{-1}$	k_{-E} $s^{-1}M^{-1}$	Std.dev.
a	*R2*: 5.81e+09 *R7*: 9.46e+11 *R12*: 5.19e+06	*R3*: 2.86e+03 *R5*: 4.85e+02	*R8*: 3.13e+03 *R10*: 3.15e+03	*R14*: 1.40e+02 *R15*: 6.00e-01 *R16*: 3.65e+02 *R17*: 1.33e+01	*R14*: 7.18e-05 *R15*: 1.27e-03 *R16*: 2.80e-01 *R17*: 5.10e-03	0.00234
b	*R2*: 1.00e+08 *R7*: 2.07e+09 *R12*: 1.00e+07	*R3*: 2.04e+03 *R5*: 1.83e+02	*R8*: 3.13e+05 *R10*: 7.48e+04	*R14*: 2.14e+03 *R15*: 3.58e-01 *R16*: 2.22e-16 *R17*: 1.08e+01	*R14*: 1.05e-01 *R15*: 1.89e-04 *R16*: 7.31e+00 *R17*: 9.43e-07.	0.00225
c	*R2*: 5.73e+08 *R7*: 5.77e+08 *R12*: 2.90e+09	*R3*: 1.12e+04 *R5*: 5.24e+01	*R8*: 1.42e+03 *R10*: 1.24e+03	*R14*: 6.61e+02 *R15*: 2.77e+01 *R16*: 7.05e+00 *R17*: 4.04e+01	*R14*: 8.66e-03 *R15*: 2.91e-16 *R16*: 2.17e-02 *R17*: 1.17e+01	0.00219
Ref. val.	*(10÷2.5)e+09*	*(2÷7)e+03*	*(1÷3)e+03*	*(0.5÷1)e+02*	< k_E	

In Tables 2 and 3 the values of optimised kinetic constants of electron transfer reactions for the three models a, b, and c, and their order of magnitude referred in the literature [5] are presented. We must note that the referred values of these parameters have been obtained in different experimental conditions and with very different techniques. Therefore, we must be careful in their use for the validation of the models.

4. Conclusions

PS II function is highly sensitive to the environmental conditions (e.g., pollutants, heat and water stress, excess light, and increasing carbon-dioxide). Therefore, the O-J-I-P fluorescence induction curve, which can be considered as a monitor of PS II, is expected to be very useful in plant biology research, and related areas such as ecology, horticulture, agronomy, and biotechnology. Specific processing and interpretation of experimental data have been proposed in our laboratory (i.e. the so-called JIP-Test) and have been successfully used in the analysis of the physiology of the plants [8,15]. To complement the JIP-Test, we propose here a way to measure and compare, *in vivo*, the degree of PS II grouping. The curvature constant C, and the overall probability of the connectivity between PS II units p, can be obtained by using a few points of the transient: F_0 at 0.05 ms, F at 0.1 ms, F at 0.3 ms, F_J at 2 ms, and F_M, by using the following relationships:

$$C = \frac{W_E - W}{V_J W (1 - W_E)} \tag{16}$$

and

$$p = \frac{F_{0.05ms}}{F_M - F_{0.05ms}} C \tag{17}$$

where:

$V_J = (F_{2ms} - F_{0.05ms}) / (F_M - F_{0.05ms})$

$W = (F_{0.1ms} - F_{0.05ms}) / (F_{2ms} - F_{0.05ms})$

$W_E = 1 - [(F_{2ms} - F_{0.3ms}) / (F_{2ms} - F_{0.05ms})]^{1/5}$

We have tried our new method on control and DCMU-treated leaves, and we have obtained very well correlated values: $C_{control} = C_{DCMU} = 0.98$, $p_{control} = 0.25$ and $p_{DCMU} = 0.26$ (see Table 1).

For any sample the degree of connectivity is unpredictable if not measured and calculated. However, all simulations and fittings of fluorescence data are compared with biochemical redox models. For this reason one usually assumes the approximation that the relative variable fluorescence $V(t)$ is equal to the fraction of closed reaction centres $B(t)$. Considering the existence of energetic cooperativity (or energetic grouping) $V(t)$ can only be transformed to $B(t)$ by knowing the constant C of the hyperbolic relationship (1). Figure 4 shows how much the kinetics $V(t)$ differs from $B(t)$ by using a probability of energetic cooperativity of only 0.17.

All three different models considered here can simulate and fit the experimental fast fluorescence induction curves in a satisfactory way. This shows clearly that for such a complex biological system the use of several different experimental methods, not only

the fluorescence data, are necessary to distinguish the best one between them. The results show that such additional experimental data can be obtained by measuring the kinetics of all (or some) redox forms presented in Figure 3, as their contribution to the fluorescence curve are very specific for every model (see Figure 4).

In a more developed model the influence of the S-states of the water splitting system will be included, because these states indeed affect the fluorescence emission [11].

Acknowledgments. This work was supported by Swiss National Foundation - Grant No. 3100 – 057046.99/1.

References

1. **Danielius RV, Satoh K, van Kan PJM, Plijter JJ, Nuijs AN, van Gorkom HJ** (1987) The primary reaction of Photosystem II in D1-D2-cytochrome b-559 complex. FEBS Lett 213: 241-244
2. **Diner BA, Babcock GT** (1996) Structure, dynamics, and energy conversion efficiency in Photosystem II. In: Ort DR & Yokum CF, eds, Advances in Photosynthesis, Vol 4: Oxygenic Photosynthesis: The Light Reactions, Kluwer Acad Publ, pp 213-247
3. **Duysens LNM, Sweers HE** (1963) In: Studies on Microalgae and Photosynthetic Bacteria, Japanese Society of Plant Physiologists, ed, Univ Tokyo Press, Tokyo, pp 353-372
4. **Govindjee** (1995) Sixty-three years since Kautsky: chlorophyll *a* fluorescence. Aust J Plant Physiol 22: 131-160
5. **Haumann M, Junge W** (1996) Protons and charge indicators in oxygen evolution In: Ort DR & Yokum CF, eds, Advances in Photosynthesis, Vol 4: Oxygenic Photosynthesis, The light Reactions, Kluwer Acad Publ, pp 165-192
6. **Hooke R, Jeeves TA** (1961) 'Direct search' solution of numerical and statistical problems. J Assoc Computing Machinery 8: 212-229
7. **Joliot A, Joliot P** (1964) Étude cinétique de la réaction photochimique libérant l'oxygène au cours de la photosynthèse. CR Acad Sci Paris 258: 4622-4625
8. **Krüger HJ, Tsimilli-Michael M, Strasser RJ** (1997) Light stress provokes plastic and elastic modifications in structure and function of photosystem II in camellia leaves. Physiol Plant 101: 265-277
9. **Lavergne J, Trissl H-W** (1995) Theory of fluorescence induction in photosystem II: Derivation of analytical expressions in a model including exciton-radical-pair equilibrium and restricted energy transfer between photosynthetic units. Biophys J 68: 2474-2492
10. **Mendes P, Kell DB** (1998) Non-linear optimization of biochemical pathways: applications to metabolic engineering and parameter estimation. Bioinformatics 14: 869-883
11. **Srivastava A, Strasser RJ, Govindjee** (1999) Greening of peas: parallel measurements of 77 K emission spectra, OJIP chlorophyll a fluorescence transient, period four oscillation of the initial fluorescence level, delayed light emission, and P700*. Photosynthetica 3: 365-392

12. **Stirbet AD, Govindjee, Strasser BJ, Strasser RJ** (1998) Chlorophyll *a* fluorescence induction in higher plants: Modelling and numerical simulation. J Theor Biol 193: 131-151
13. **Stirbet AD, Rosenau Ph, Ströder AC, Strasser RJ** (1999) Fast Chl *a* fluorescence induction models. Parameter optimisation study. In: Proc 3rd Intern Symp Mathematical Modelling and Simulation in Agriculture & Bio-Industries, Uppsala, Sweden
14. **Stirbet AD, Strasser RJ** (1995) Numerical simulation of the fluorescence induction in plants. Archs Sci Genève 48: 41-60
15. **Strasser BJ, Strasser RJ** (1995) Measuring fast fluorescence transients to address environmental questions: The JIP-Test. In: Mathis P, ed, Photosynthesis: from Light to Biosphere, Kluwer Acad Publ, pp 977-980
16. **Strasser RJ** (1981) The grouping model of plant photosynthesis: heterogeneity of photosynthetic units in thylakoids. In: Akoyunoglou G, ed, Structure and Molecular Organization of the Photosynthetic Apparatus, Philadelphia: Balaban International Science Service, pp 727-737
17. **Strasser RJ** (1978) The grouping model of plant photosynthesis. In: Akoyunoglou G & Argyroudi-Akoyunoglou JH, eds, Chloroplast Development, Elsevier, Holland, pp 513-524
18. **Strasser RJ, Srivastava A, Govindjee** (1995) Polyphasic chlorophyll *a* fluorescence transient in plants and cyanobacteria. Photochem Photobiol 61: 32-42
19. **Vredenberg WJ** (2000) A 3-state model for energy trapping and fluorescence in PSII incorporating radical pair recombination. Biophys J 79: 25-38